

# Performance Analysis of Shunt Active Power Filter using PLL based Control Algorithms Under Distorted Supply Condition

Rajesh K Patjoshi

Electronics and Communication Engg.Dept.  
National Institute of Technology  
Rourkela, India  
rajeshpatjoshi1@gmail.com

Kamala kanta Mahapatra

Electronics and Communication Engg.Dept.  
National Institute of Technology  
Rourkela, India  
Kmaha2@gmail.com

**Abstract**— This paper presents three different PLL based control algorithms for shunt active Power filter (SAPF) under the distorted supply condition. Different synchronisation techniques such as Modified SRF (MSRF-PLL), Transformation angle detector and SRF based PLL have been applied to SAPF and analyzed under different distortion conditions of supply voltage. From the simulation results, it is found that the MSRF-PLL achieves better performance as compared to other two standard PLL techniques on the basis of THD% (total harmonic distortion). The MSRF-PLL is fast in transient response and robust against disturbances on the grid voltage wave. Here simulation has been carried out using MATLAB under distorted line voltage conditions.

**Index Terms**— Modified SRF, Angle Detector SRF, SRF PLL, harmonic distortion, distorted line voltage.

## I. INTRODUCTION

Interfacing of power electronics converters to the supply line, particularly for the medium and high power line requires proper synchronization for the purpose of better operation and control of power electronics based equipments[1].The synchronization is based on considering the phase angle of supply voltage and current .The signal in the utility are often corrupted by power line disturbances such as harmonics, voltage sag and swell, phase jump, commutation notch and unbalanced conditions[2]–[4].The phase-angle of the voltage/current fundamental component at the point of common coupling (PCC) should be tracked online in order to control the energy transfer between the active power filter and the ac mains., so suitable synchronization algorithms have been evolving for proper operation of the active power filter. The P-Q operation point of active power filter depends on the phase angle of the utility. In general, the controllers of power electronic converters implement synchronization algorithms to assess exchanges of electrical energy. Measurements at the PCC are made in order to estimate voltage/current absolute phase-angles. The PLL control algorithms were considered for three-phase electric systems, Kaura at [5], and he established a PLL technique for Synchronous Reference Frame, which provided good performance and fast transient response under

less distortion level and small unbalance condition. Any condition different from these specifications provides poor phase synchronization, lock loss, distorted output signal resulting in uncorrected harmonic compensation. Utility connected systems such as UPS, PWM rectifiers and Active Power Filters have its performance depends on PLL accuracy, especially those in which the controllers are based on SRF.

An open loop system, named low-pass transformation angle detector, was able to synchronize with the positive-sequence of the fundamental vector of a three-phase voltage/current system, presented in [6]. This system was proposed as a Transformation Angle Detector PLL .

The PLL Algorithm proposed in [7], was based on Modified Synchronous Reference Frame technique (MSRF) and offers quickly lock feature without PI controller and uses only phase-A voltage measurement by reducing sensors even if in three phase utility case. Also, voltage unbalance and harmonic do not disturb the performance of the PLL.

This paper presents three different topologies of PLL such as Modified SRF (MSRF-PLL), Transformation Angle Detector, and SRF based PLL for detection of positive sequence signal from the distorted supply voltage for proper operation of the active power filter. Here three different distorted conditions of supply voltage have been considered in comparative analysis of the above mentioned PLL structures. Comparison result shows the superiority of MSRF-PLL as compared to others on the basis of THD% (total harmonic distortion).

## II. CONTROL STRUCTURE OF PLL SYSTEM

Various methods of synchronization techniques are outlined in this section. They are categorized as open-loop and closed-loop methods. Open-loop methods directly estimate the phase angle of the voltage and current signal based on frame signal. In closed-loop methods, while the frame voltages are being processed, the estimation of the phase is adaptively updated through a loop mechanism. This loop is aimed at locking the estimated value of the phase angle to its actual value. The paper considers both open and closed loop PLL control techniques for synchronization of the active power

filter. In open loop technique, the Transformation Angle Detector and in the close loop system, both SRF PLL and Modified SRF (MSRF-PLL) are used.

#### A. Open-Loop Synchronization Method

Transformation Angle Detector is considered here for three-phase active power filter connected to the utility grid. The performance of this synchronization method is analyzed under distorted grid voltages. Fig. 1 shows the control scheme of the Transformation Angle Detector. A three-phase system voltages ( $V_a, V_b, V_c$ ) are transformed to its equivalent *Clarke's Transformation* (transformation from abc to  $\alpha\beta$ ).

$$\begin{bmatrix} \alpha \\ \beta \end{bmatrix} = \begin{bmatrix} 1 & -1/2 & -1/2 \\ 0 & \frac{\sqrt{3}}{2} & -\frac{\sqrt{3}}{2} \end{bmatrix} \quad (1)$$

It is assumed that there is no negative-sequence of fundamental frequency and the phase angle of the positive-sequence is estimated from  $\hat{V}_{\alpha 1}$  and  $\hat{V}_{\beta 1}$ , which are obtained by filtering harmonics from  $V_\alpha$  and  $V_\beta$  through ordinary low-pass filters (LPFs). The filtered signals are normalized and passed through the rotation matrix to compensate for the phase lag due to the LPFs. In designing LPFs, a tradeoff should be made between robustness and transient convergence speed. The smaller cutoff frequency of the filters results in less distortion in the estimated angle. However, this results in a slower rate of convergence. A major deficiency of this method is its sensitivity to the grid frequency deviations [8]. If the center frequency varies, there is no control on the phase lag introduced by the LPFs and hence its full compensation is not possible. Another shortcoming of the LPF-based method is its sensitivity to voltage unbalance. To overcome this downside, the following two methods are approached.

#### B. Closed-Loop Synchronization Method

A closed-loop method operates on regulating an error signal to zero. Here both SRF PLL and MSRF-PLL are considered for synchronization.

##### 1) Synchronization Based on SRF PLL

Synchronous reference frame strategy is a popular method used in the generation of the current reference by co-ordinate transformations. For this purpose, it employs the well known *Clarke's Transformation* (transformation from abc to  $\alpha\beta$ ) and *Park's Transformation* (transformation from  $\alpha\beta$  to dq), which are shown graphically in Fig.2.

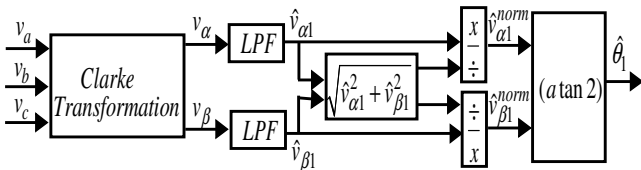


Fig.1 Control scheme of the Transformation Angle Detector

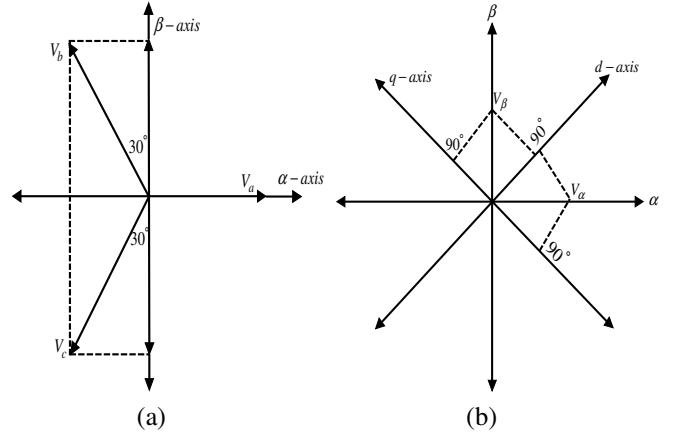


Fig.2(a) Clarke' Transformation, (b) Park's Transformation

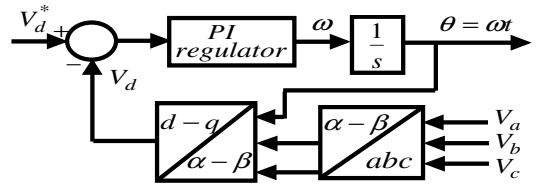


Fig.3 SRF based PLL structure

Operation of a three phase SRF based PLL can be schematically shown in the Fig.3. To obtain the phase information, the three phase voltage signals ( $V_a, V_b, V_c$ ) are first transferred into stationary two phase systems ( $V_\alpha$  and  $V_\beta$ ) and further transferred into synchronously rotating reference frame ( $V_d$  and  $V_q$ ).

Where,

$$V_a = V_m \sin \omega t \quad (2)$$

$$V_b = V_m \sin(\omega t - 120^\circ) \quad (3)$$

$$V_c = V_m \sin(\omega t + 120^\circ) \quad (4)$$

$$V_\alpha = V_a - \frac{1}{2}V_b - \frac{1}{2}V_c \quad (5)$$

$$V_\beta = \frac{\sqrt{3}}{2}V_c - \frac{\sqrt{3}}{2}V_b \quad (6)$$

$$V_d = V_\alpha \cos \theta + V_\beta \sin \theta \quad (7)$$

$$V_q = V_\beta \cos \theta - V_\alpha \sin \theta \quad (8)$$

Now phase angle ( $\theta$ ) can be obtained by setting the reference  $V_d^*$  equal to zero and compared with  $V_d$ . The PI controller ( $K_p \cdot \frac{1+s\tau}{s\tau}$ ) is used to regulate this d-component and the output of this PI controller is the grid

frequency. After the integration of the grid frequency, the utility voltage angle is obtained. As  $\omega t$  is the angular frequency,  $\sin \omega t$  is in phase with the fundamental of the  $\alpha$ -component and the  $\cos \omega t$  is  $90^\circ$  phase-shift with the  $\beta$ -component. The controller gains are designed such that  $V_d$  follows the reference value and the estimated phase angle ( $\phi$ ) should be equal to the phase angle ( $\theta$ ). Now if  $\theta \approx \phi$  then the space vector of voltage gets aligned to d axis.

## 2) Synchronization Based on Modified SRF(MSRF-PLL)

The PLL algorithm [9] is designated as modified SRF-PLL (MSRF-PLL) because it considers only one phase voltage (i.e.,  $V_a$ ) wave in place of three phase voltage waves used in the SRF-based algorithms. The PI control in the SRF PLL control loop is eliminated by MSRF PLL, because the PI controller used in SRF PLL gets sluggish under highly distorted utility condition.

The MSRF-PLL uses an algorithm which is based upon the principle of Coulon oscillator [10]. Block diagram of the Coulon oscillator is shown in Fig. 4, where the input signal  $x(t)$  is harmonically rich, and is given by

$$x(t) = \sum_{i=1}^N A_i \sin(\omega_i t + \phi_i) \quad (9)$$

Where  $N$  is the harmonic order,  $A_i$  is the harmonic amplitude, and  $\phi_1$  is the phase angle. The Coulon oscillator frequency is defined as  $f_r = \omega_r/2\pi$ , which generates the  $\sin(\omega_r t)$  and  $\cos(\omega_r t)$  signals. Therefore, after multiplication with the signal  $x(t)$ , it generates two corresponding signals  $x_1(t)$  and  $x_2(t)$  respectively, by

$$x_1(t) = \sum_{i=1}^N A_i \sin(\omega_i t + \phi_i) \cdot \sin(\omega_r t) \quad (10)$$

$$x_2(t) = \sum_{i=1}^N A_i \sin(\omega_i t + \phi_i) \cdot \cos(\omega_r t) \quad (11)$$

Eq.(10) & (11) can be written as

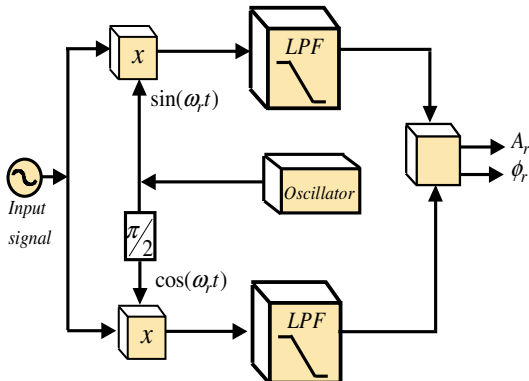


Fig.4 Block Diagram of Coulon Oscillator

$$x_1(t) = \sum_{i=1}^N \frac{A_i}{2} \{ \cos[(\omega_i - \omega_r)t + \phi_i] - \cos[(\omega_i + \omega_r)t + \phi_i] \} \quad (12)$$

$$x_2(t) = \sum_{i=1}^N \frac{A_i}{2} \{ \sin[(\omega_i - \omega_r)t + \phi_i] + \sin[(\omega_i + \omega_r)t + \phi_i] \} \quad (13)$$

By taking  $f_1 = \omega_1/2\pi$ , and  $\omega_i = i\omega_1$ ,  $\omega_r = r\omega_1$  ( $i$  and  $r$  are harmonic orders), Eq(12) and (13) can be expressed as

$$x_1(t) = \sum_{i=1}^N \frac{A_i}{2} \{ \cos[(i-r)\omega_1 t + \phi_i] - \cos[(i+r)\omega_1 t + \phi_i] \} \quad (14)$$

$$x_2(t) = \sum_{i=1}^N \frac{A_i}{2} \{ \sin[(i-r)\omega_1 t + \phi_i] + \sin[(i+r)\omega_1 t + \phi_i] \} \quad (15)$$

In order to extract the fundamental frequency of  $x(t)$  the oscillator frequency  $\omega_i$  should be tuned to be the same frequency as  $\omega_1$ , i.e.,  $r = i = 1$ . Therefore,

$$x_1(t) = \frac{A_1}{2} \cos(\phi_1) - \frac{A_1}{2} \cos(2\omega_1 t + \phi_1) + \sum_{i=2}^N \frac{A_i}{2} \{ \cos[(i-1)\omega_1 t + \phi_i] + \cos[(i+1)\omega_1 t + \phi_i] \} \quad (16)$$

$$x_2(t) = \frac{A_1}{2} \sin(\phi_1) - \frac{A_1}{2} \sin(2\omega_1 t + \phi_1) + \sum_{i=2}^N \frac{A_i}{2} \{ \sin[(i-1)\omega_1 t + \phi_i] + \sin[(i+1)\omega_1 t + \phi_i] \} \quad (17)$$

First term of the equation (16) and (17) is the DC component related to the fundamental magnitude  $A_1$  and phase angle  $\phi_1$ , and the second term relates to the second harmonic component, and the remaining terms in the equation are higher frequency components. A low-pass filter, filters out the DC component of each signal which are given as

$$V_d' = \frac{A_1}{2} \cos \phi_1 \quad (18)$$

$$V_q' = \frac{A_1}{2} \sin \phi_1 \quad (19)$$

Therefore, the output of the Coulon oscillator can be derived as

$$A_1 = \sqrt{(2V_d')^2 + (2V_q')^2} \quad (20)$$

$$\phi_1 = \tan^{-1} \left( \frac{V_q'}{V_d'} \right) \quad (21)$$

When the phase of the oscillator coincides with the phase of the fundamental component of input signal  $x(t)$  i.e.,  $\phi_1 = 0$ , then  $V_d' = 0.5A_1$  and  $V_q' = 0$ . It can be shown that the Coulon oscillator not only filter out the fundamental component of the input signal, but also other harmonic components can be filtered out by appropriately tuning of the coupled oscillator.

Fig.5 shows the block diagram of the MSRF PLL structure, where  $V_{sa}$  is the phase A utility voltage at 50Hz, and  $V_d$ ,  $V_q$  can be expressed as

$$V_d = 2V_d' = A_1 \cos \phi_1 \quad (22)$$

$$V_q = 2V_q' = A_1 \sin \phi_1 \quad (23)$$

Where  $\phi_1 = \arcsin(V_q)$  and  $A_1 = 1.0$ .

The phase angle  $\phi_1$  of the output can be fed back to the oscillator to lock its frequency and phase so that  $\phi_1$  approaches to zero. In this condition,  $\sin(\omega_e t)$  and  $\cos(\omega_e t)$  can be defined as unit phase voltage  $V_{sa}$ . The advantage of the MSRF-PLL in comparison with the SRF-based scheme is that it is derived from only one phase voltage, and the unit vector output is not affected by harmonic distortion, unbalance or sag/swell of the utility voltage.

### III. FUNCTIONAL STRUCTURE OF SAPF

The complete control structure of SAPF is shown in Fig.6. The d-axis load current when high pass filtered (DC alone removed) will give the harmonic content of the load current, and the q-axis load current gives the reactive content of the load current. The outputs of the d and q axis current controllers are added to the inverter d and q-axis currents respectively to get current references required for generation of the gating pulses, The output of the voltage controller represents the active current requirement of the active power filter to compensate for the various losses.

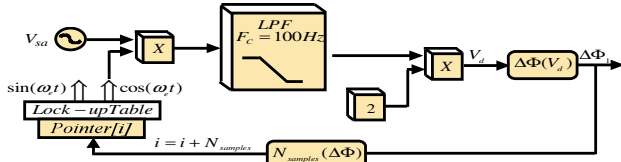


Fig.5 Block diagram of the MSRF PLL structure

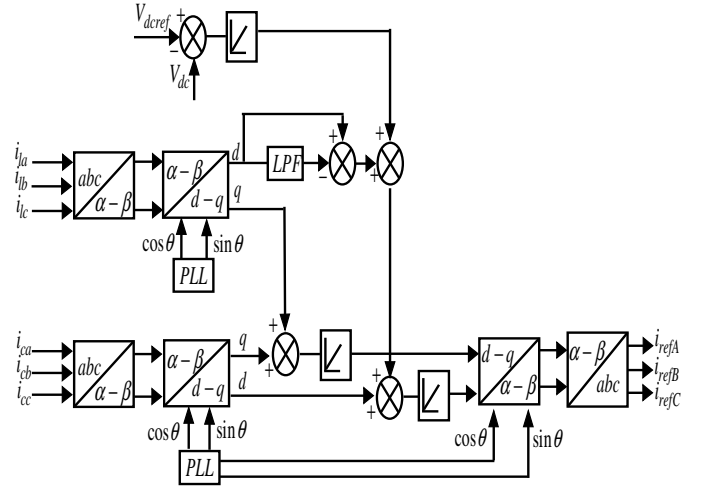


Fig.6 Functional Structure of SAPF

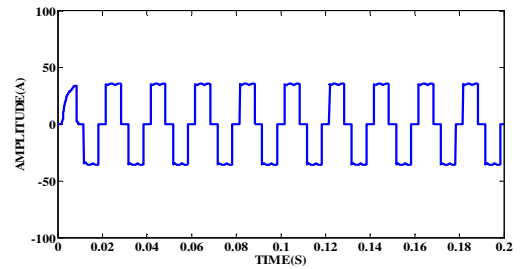
### IV SIMULATION RESULTS AND DISCUSSIONS

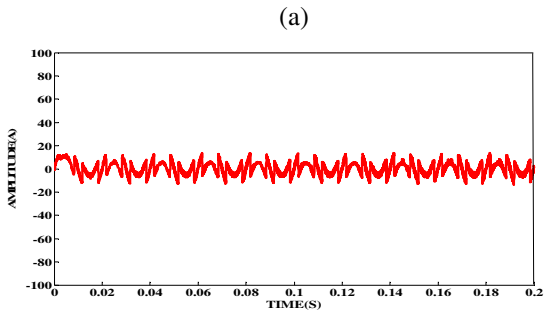
The performance of the SAPF with different PLL structured such as a Transformation Angle Detector, SRF-PLL and Modified SRF (MSRF-PLL) is evaluated through MATLAB programming in order to model and test the system.

To verify the SAPF with different PLL structures, the parameter values considered here are; Line to line source voltage (100 V, 50 Hz), Source impedance of  $R_s$  and  $L_s$  (0.1  $\Omega$  and 0.15 mH), the Filter impedance of  $R_c$  and  $L_c$  (0.1  $\Omega$  and 0.7 mH); Load impedance of  $R_L$  and  $L_L$  (10 $\Omega$  and 20 mH), DC side capacitance  $C_{DC}$  (2000  $\mu$ F). The power devices are built by IGBT with anti parallel diodes. The simulation is executed under steady state using diode rectifier with RL load.

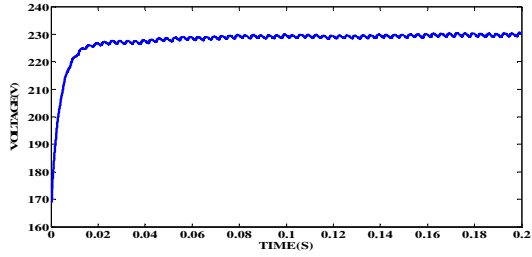
The simulation results for load current, compensating current, capacitor voltage, and source current waveforms at low distortion (0.0108%) of line voltage are shown in Fig.7. From Table I, it is shown that the performances of all three PLL structures (TAD, SRF-PLL, and MSRF-PLL) are nearly same as a low distortion condition of supply voltage. Fig. 8 shows the source current waveforms, which are in phase with the source voltage for the above PLL structures in medium distortion (7.99%) condition, but MSRF-PLL gives slightly better performance according to THD% calculation.

The source current waveforms along with their spectrums for TAD,SRF-PLL and MSRF-PLL methods in high distortion (19.99%)condition of supply voltage are shown in Fig.9,10 and 11 respectively. Table I shows that MSRF-PLL (THD-11.90%) is found to be much better than the other two methods.

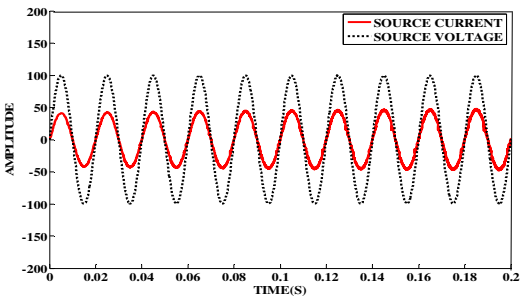




(a)

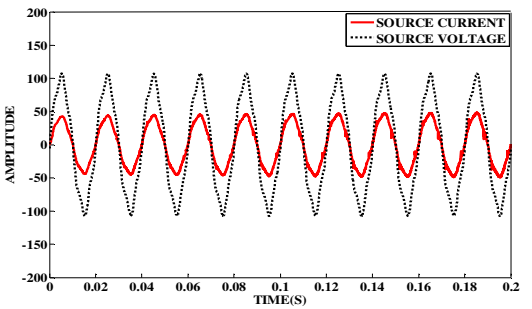


(b)

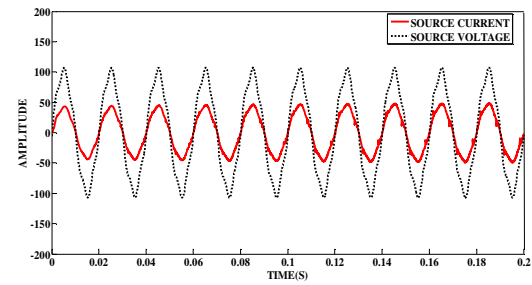


(c)

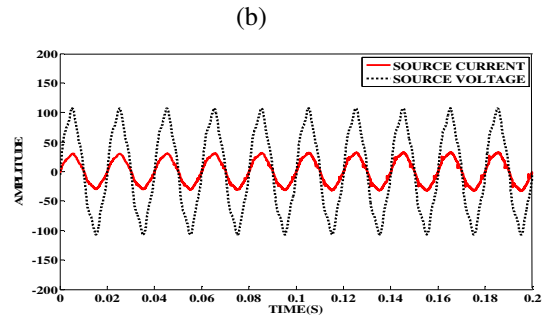
Fig.7(a)Load current,(b)Compensating current,(c) Capacitor voltage,(d)Source voltage & source current waveforms after compensation for low distortion condition.



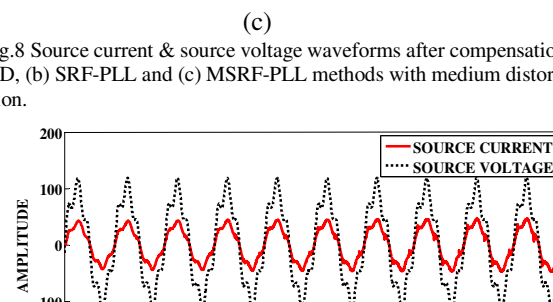
(d)



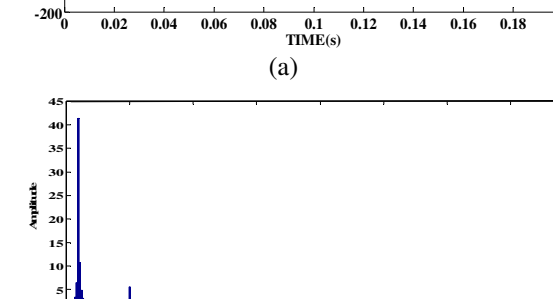
(e)



(a)

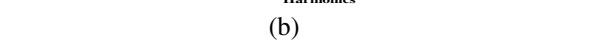


(b)



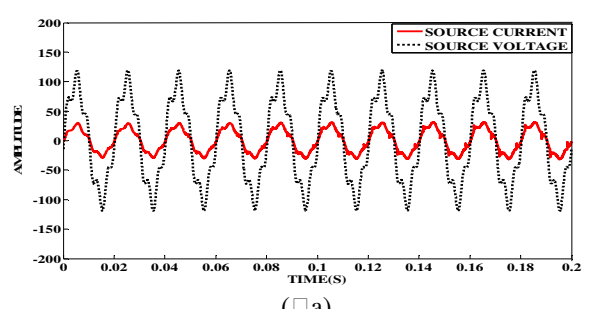
(c)

Fig.8 Source current & source voltage waveforms after compensation for (a) TAD, (b) SRF-PLL and (c) MSRF-PLL methods with medium distortion condition.

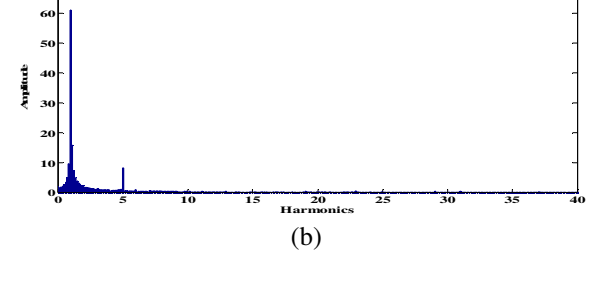


(a)

Fig.9(a) Source current & source voltage waveform, (b) Source current spectrum after compensation for TAD method with high distortion condition.

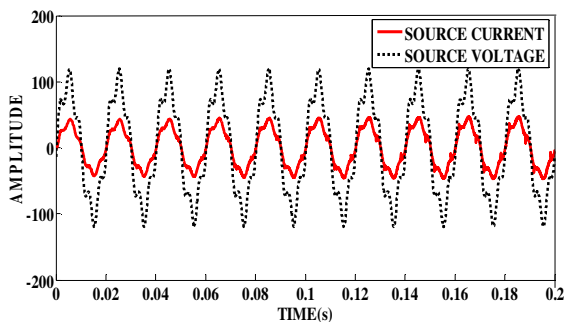


(b)

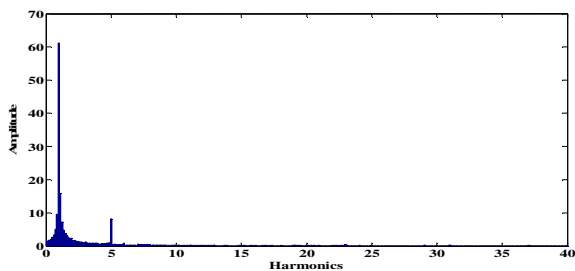


(c)

Fig.10 (a) Source current & source voltage waveform, (b) Source current spectrum after compensation for SRF-PLL method with high distortion condition.



(a)



(b)

Fig.11 (a) Source current & source voltage waveform, (b) Source current spectrum after compensation for MSRF-PLL method with high distortion condition.

## V.CONCLUSIONS

Harmonic current compensation for SAPF has been performed using TAD, SRF-PLL and MSRF-PLL based synchronization methods. Three different distorted conditions (0.0188, 7.99 and 19.99%) THD of supply voltage have been considered for comparative analysis of the above mentioned PLL structures.

From the simulation results, it is found that the MSRF-PLL achieves better performance as compared to other two standard PLL techniques on the basis of THD% (total harmonic distortion). The superiority of MSRF-PLL is proved in all three distorted conditions of line voltage. The MSRF-PLL is fast in transient response and robust against disturbances on the grid voltage wave.

## REFERENCES

- [1] J. Svensson, "Synchronization methods for grid-connected voltage source converters," in *Proc. Inst. Elect. Eng. Generation, Transmission, Distribution*, vol. 148, May 2001, pp. 229–235.
- [2] Gary W. Chang, "A novel reference compensation current strategy for shunt active power filter control," *IEEE Trans. power delivery*, vol. 19, no.4, pp.1751-1758, Oct. 2004.
- [3] Hilmy Awad, "Operation of static series compensator under distorted utility conditions," *IEEE Trans. power systems*, vol. 20, no.1, pp.448-457, Feb. 2005.
- [4] Christoph Meyer, "Optimized control strategy for a medium-voltage DVR—theoretical investigations and experimental results," *IEEE Trans. Power Electron*, vol. 23, no.6, pp.2746-2754, Nov. 2008.
- [5] V. Kaura and V. Blasko, "Operation of a phase locked loop system under distorted utility conditions," *IEEE trans. on Industry Applications*, Vol.33, no. 1, pp. 58-63, 1997.
- [6] R. F. de Camargo and H. Pinheiro, "Synchronisation method for Three-phase PWM converters under unbalanced and distorted grid," *Electric Power Applications, IEEE Proceedings -*, vol. 153, no. 5, pp. 763–772, Sep. 2006.
- [7] Carlos Henrique da Silva, "A digital PLL scheme for three-Phase system using modified synchronous reference frame," *IEEE Trans. Ind. Electron.*, vol. 57, no. 11, pp.3814–3821, Nov. 2010.
- [8] Masoud Karimi, "A Method for Synchronization of Power Electronic Converters in Polluted and Variable- Frequency Environments," *IEEE Trans. Power Syst.*, vol.19, no.3, pp.1263-1270, Aug.2004.
- [9] Carlos Henrique da Silva, "DSP Implementation of Three-Phase PLL using Modified Synchronous Reference Frame," in *IEEE industrial electronics society*, pp.1697-1701, Nov.2007.
- [10] S. Tnani, M. Mazaudier, A. Berthon, and S. Diop, "Comparison between different real-time harmonic analysis methods for control of electrical machines," in *Proc. PEVD*, 1994, pp. 4946–4951.

TABLE I  
(THD% COMPARISON OF PLL METHODS)

Source Voltage (THD%)	Synchronization Method	Source Current Before Compensation (THD%)	Source Current After Compensation (THD%)
0.0188	TAD	31.1422	4.5100
	SRF-PLL	31.1422	4.4707
	MSRF-PLL	31.1422	4.3028
7.99	TAD	31.1422	7.3142
	SRF-PLL	31.1422	7.1093
	MSRF-PLL	31.1422	6.8120
19.99	TAD	31.1422	14.2875
	SRF-PLL	31.1422	13.8813
	MSRF-PLL	31.1422	12.9952